

# FORGE

## Fate Of Repository Gases

European Commission FP7

European Commission

# State of the Art - Experiment Specifications and Validation of Experimental Devices

FORGE Report D2.1– VER.0

	Name	Organisation	Signature	Date
Compiled	Virginie Wasselin–Trupin	IRSN		19 <sup>th</sup> April 2010
Verified				
Approved				

Euratom 7<sup>th</sup> Framework Programme Project: FORGE



## Fate of repository gases (FORGE)

The multiple barrier concept is the cornerstone of all proposed schemes for underground disposal of radioactive wastes. The concept invokes a series of barriers, both engineered and natural, between the waste and the surface. Achieving this concept is the primary objective of all disposal programmes, from site appraisal and characterisation to repository design and construction. However, the performance of the repository as a whole (waste, buffer, engineering disturbed zone, host rock), and in particular its gas transport properties, are still poorly understood. Issues still to be adequately examined that relate to understanding basic processes include: dilational versus visco-capillary flow mechanisms; long-term integrity of seals, in particular gas flow along contacts; role of the EDZ as a conduit for preferential flow; laboratory to field up-scaling. Understanding gas generation and migration is thus vital in the quantitative assessment of repositories and is the focus of the research in this integrated, multi-disciplinary project. The FORGE project is a pan-European project with links to international radioactive waste management organisations, regulators and academia, specifically designed to tackle the key research issues associated with the generation and movement of repository gasses. Of particular importance are the long-term performance of bentonite buffers, plastic clays, indurated mudrocks and crystalline formations. Further experimental data are required to reduce uncertainty relating to the quantitative treatment of gas in performance assessment. FORGE will address these issues through a series of laboratory and field-scale experiments, including the development of new methods for up-scaling allowing the optimisation of concepts through detailed scenario analysis. The FORGE partners are committed to training and CPD through a broad portfolio of training opportunities and initiatives which form a significant part of the project.

Further details on the FORGE project and its outcomes can be accessed at [www.FORGEproject.org](http://www.FORGEproject.org).

### Contact details:

**Virginie Wasselin–Trupin**

**Organisation** IRSN

Tel: (33)1 58 35 86 85

Fax (33)1 58 35 79 76

email: [virginie.wasselin-trupin@irsn.fr](mailto:virginie.wasselin-trupin@irsn.fr)

web address: [www.irsn.org](http://www.irsn.org)

Address IRS[N] DSU/SSIAD/BECID

BP 17

92262 Fontenay aux Roses

# Contents

<b>Contents.....</b>	<b>ii</b>
<b>Introduction .....</b>	<b>1</b>
1.1 Corrosion .....	1
1.1.1 Corrosion mechanisms of iron and carbon steels .....	1
1.1.2 Carbon steel corrosion and hydrogen evolution rates under repository conditions 4	
1.1.3 Conclusions.....	8
1.1.4 Literature .....	8
1.2 Corrosion under radiation .....	11
1.2.1 Radiolysis of solutions .....	11
1.2.2 Radiolysis modelling.....	13
1.2.3 Influence of radiation on corrosion.....	14
1.2.4 Conclusion .....	16
1.2.5 Literature:.....	16
<b>Annexes.....</b>	<b>19</b>

# Introduction

It is well known that the largest source of gas in a repository will come from anaerobic corrosion of iron canisters. Despite a huge number of publications devoted to the study of iron and carbon steel corrosion mechanisms under various conditions, there are a lot of uncertainties concerning hydrogen evolution rate in a repository from this source. Especially, there are some discrepancies in respect of the effect of content of oxygen, carbon oxide, or chemistry of groundwater. There is very little information on the effect of radiation on mechanism of iron corrosion in anaerobic conditions and hydrogen evolution rate.

## 1.1 CORROSION

This part of the state of the art report is devoted to the review of known information on iron corrosion in respect to hydrogen evolution rate. It will serve primarily for interpretation of experimental results, which are focused on measuring of hydrogen evolution rate under various conditions from iron and carbon steel corrosion.

### 1.1.1 Corrosion mechanisms of iron and carbon steels

The character of corrosion mechanisms of iron and carbon steels depends primarily on the content of oxygen in a groundwater contacting canisters. From this point, DGR evolution phases can be divided as follows:

- **Aerobic phase** - during the operation phase of a repository and some time after its closure, the overall aerobic corrosion reactions will occur in the unlimited presence of oxygen trapped in the buffer and backfill materials with sufficient flux of oxygen from unsaturated environment (~8 ppm of O<sub>2</sub>). No hydrogen is generated in the phase.
- **Limited flux of oxygen** – phase (0.03 – 8 ppm of O<sub>2</sub>) the buffer is assumed to be saturated with groundwater, so that the mass transport of oxygen to and from the canister surface is by diffusion through water-filled pores. Hydrogen can be generated depending on the contact of oxygen in groundwater.
- **Anaerobic phase** - after consumption of oxygen (< 0.03 ppm of O<sub>2</sub>). Corrosion is connected with hydrogen generation.

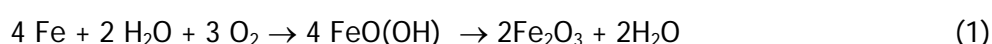
The time scales of the individual phases will depend on the host rock environment and the design of the repository.

#### 1.1.1.1 AEROBIC PHASE

Corrosion of canisters starts immediately after their manufacture in the atmosphere of storage facilities. The character of corrosion mechanism will depend primarily on the humidity of the air in storage facilities. After achieving so-called “critical relative humidity” (CRH), a continuous film can be formed on metal and corrosion goes in aqueous phase. Achieving of CRH depends on the type of metal, and other conditions. Dry oxidation phase leads to the steady build up of an oxide layers. In general, the thicker is the oxide layer, the slower is the subsequent oxidation rate. The detailed character of oxide layer depends, however, on the content of air contaminants: mainly the content of sulphur and nitrogen oxides.

After achieving critical relative humidity, corrosion of carbon steels goes in aqueous phase and is 10 to 100 times higher than corrosion in dry phase. In bentonite environment, the critical relative humidity will be achieved very quickly.

The corrosion of iron in pure water under aerobic conditions can be expressed by the following equation:



It is supposed that no hydrogen is formed under this phase. From thermodynamic point of view the driving force (Gibbs energy = -1374 kJ/mol) of this reaction is very favourable and the reaction is thus practically irreversible. The solubility of formed iron-oxyhydroxides and iron oxides is very low and if no constant removing of solid products would proceed, the general corrosion rate would very quickly slow down due to corrosion products constraints.

Under some conditions, primarily a high redox potential difference, very adherent and covering solids may be formed on the surface of iron, especially in the alkaline environment. These solid products will passivate the metal and the corrosion will practically decrease to negligible values. The presence of carbonates can contribute significantly to the formation of passive layers on the surface of iron. Problem is that a passive film formed can be breached resulting in localized forms of degradation, such as pitting, crevice corrosion, stress-corrosion cracking (SCC), or hydrogen embrittlement (HE). The rate of localized corrosion is of rates many orders of magnitude higher than the rate of general corrosion. The tendency of iron to passivation depends primarily on the iron additives. Passivation layers are formed very quickly if the content of Cr is higher than 12 %. To the formation of passivation layers contributes also elements like Mo or Ni, but the anions like  $\text{Cl}^-$  or  $\text{SO}_4^{2-}$  disturb the passive layers.

#### 1.1.1.2 AQUEOUS CORROSION WITH LIMITED FLUX OF OXYGEN

After emplacement of the canisters in DGR, and after sealing all the paths to atmosphere, the bentonite will gradually saturate with water and the concentration of trapped oxygen will be reduced by corrosion and microbial reactions. It is supposed (Marsh et al., 1987) that three following sources of oxygen will be in the repository after its closure:

- The air trapped in the pore space of buffer and backfill material
- Dissolved oxygen in the groundwater permeating the repository
- Oxygen formed by radiation

It was reported (Marsh et al., 1987) that this period is indefinite if the diffusion coefficient of oxygen in bentonite is  $1.2 \times 10^{-10} \text{ m}^2 \text{ s}^{-1}$  and about 130 years if the diffusion coefficient is  $1.2 \times 10^{-11} \text{ m}^2 \text{ s}^{-1}$ . The authors, however, assume - very conservatively - that the concentration of oxygen at the floor of repository tunnels remains very high (8 ppm) and constant. This condition is however, as was shown in recent REX project (Puigdomenech et al., 2000, 2001), unrealistic high mainly due to microbial consumption of oxygen during its way to deep groundwater.

In the bentonite environment, diffusion coefficient of oxygen is decreasing with bentonite density according to Manaka, 2000 (Fig. 1) and therefore the effect of oxygen reactions will quickly decrease.

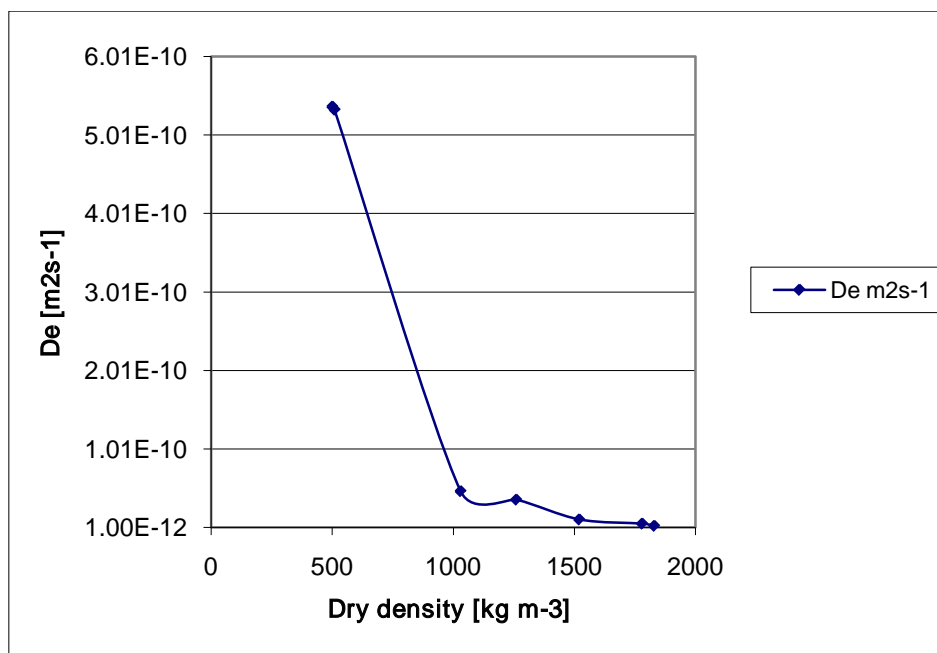


Figure 1: The change of diffusion coefficient for oxygen on density of bentonite

It is supposed that only under the presence of oxygen, a sufficiently high potential might be generated leading to the passivation of carbon steel surface and possible localized corrosion. The current approaches (Dunn et al., 2000, Druyts et al., 2001) for evaluating the tendency of iron and iron alloys (stainless steels) to localized corrosion are based on determining characteristic potentials of polarisation curves. Values of critical potential for pit nucleation ( $E_{np}$ ) and critical potential for repassivation ( $E_{pp}$ ) (protection potential) are compared with the values of corrosion (open circuit) potential ( $E_{corr}$ ). If  $E_{corr}$  exceeds  $E_{np}$ , pits will initiate and grow. If  $E_{corr}$  is between  $E_{np}$  and  $E_{pp}$  existing pits will grow but no new ones will be formed and mechanical damages to a passive layer will give rise to localised corrosion and occurring crevice corrosion will also continue. For  $E_{corr}$  below  $E_{pp}$  all pits will repassivate. It seems that in the environment without oxygen, corrosion potential  $E_{corr}$  is very low and therefore it not very probable that some type of localized corrosion could be important, but it can be supposed that a very low concentration of oxygen the passive film cannot be reproduced sufficiently and therefore the corrosion rate becomes higher.

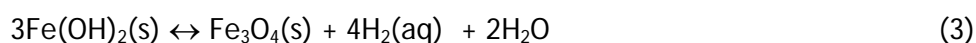
It is supposed that during this phase hydrogen can be generated by reactions described below.

#### 1.1.1.3 AQUEOUS ANAEROBIC CORROSION

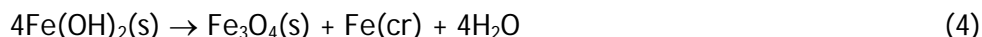
After some time depending on a number of factors, which affects decay of oxygen in surrounding environment, iron will corrode without any oxygen through the following reaction.



Ferrous hydroxide is not stable and can easily decompose by so-called Shikorr reaction to magnetite leading again to the formation of hydrogen.



Above 85 °C iron hydroxide is decomposed through the following reaction without hydrogen evolution



The Schikorr reaction is very slow under temperatures about 60 °C.

Reaction (3) is very often used for recalculation of hydrogen evolution rate from measuring corrosion rate form example by weight loss measurement. The following equation was used for recalculation of corrosion rate on hydrogen evolution rate

$$v_{\text{H}_2} = S \times R \times \rho \times m \times \frac{1}{M_{\text{Fe}} / 1000}$$

where  $v_{\text{H}_2}$  is hydrogen generation rate mol/year,  $S$  is reactive surface area ( $\text{m}^2$ ),  $R$  is corrosion rate m/year,  $\rho$  is density of iron,  $m$  is stoichiometric factor (4/3) for the generation of magnetite (equation (3)) and  $M_{\text{Fe}}$  is molecular weight of iron (55.85 g/mol).

(In some older publications the results of hydrogen evolution rate were given in  $\text{ml m}^{-2} \text{d}^{-1}$ . The rate in units of  $\text{mol m}^{-2} \text{yr}^{-1}$  can be obtained by dividing the value by number 61.41.)

### 1.1.2 Carbon steel corrosion and hydrogen evolution rates under repository conditions

A number of experiments have been devoted to the measurements of carbon steel corrosion and hydrogen evolution rates, (Jelinek, Neufeld, 1982, Simpson, 1984, Simpson et al., 1985, Anantamula et al. 1987, Marsh, Taylor, 1988, Schenk, 1988, Grauer et al., 1991, Hara et al., 1992, Honda et al., 1991, Kozaki et al., 1994, Fujisawa et al.1997, Xia et al., 2005, Smart et al., 2001, 2008), and reviews (Platts et al., 1994, Wiborgh et al., 1986 under simulated repository conditions.

Jelinek and Neufeld (1982) measured the hydrogen evolution from carbon steel in pure water or in 0.1 N  $\text{NaHCO}_3$  solution using gas chromatography methods in the temperature range between 60 and 100 °C. Various amount of copper was also added to the solution as a potential catalyst of the reactions leading to the hydrogen evolution. The results of their measurements are given in the following Table 1.

Table 1: Hydrogen formation rates at various conditions (Jelinek, Neufeld, 1982)

Solution composition	Hydrogen evolution ( $\text{molm}^{-2}\text{yr}^{-1}$ ) 60 °C	Hydrogen evolution ( $\text{molm}^{-2}\text{yr}^{-1}$ ) 80 °C	Hydrogen evolution ( $\text{molm}^{-2}\text{yr}^{-1}$ ) 90 °C	Hydrogen evolution .. ( $\text{molm}^{-2}\text{yr}^{-1}$ ) 100 °C
Distilled water	0.18	0.2	0.15	0.29
Dist. Water + 0.2 ppm Cu		0.31		
Dist. Water + 1 ppm Cu	0.38	0.20	0.07	
Dist. Water + 1 ppm Cu	0.34	0.33	0.12	
0.1 N $\text{NaHCO}_3$	0.14	0.59	0.07	
0.1 N $\text{NaHCO}_3$ + 10 ppm Cu	0.07		0.1	
0.05 N $\text{KClO}_3$	0.28			

Hydrogen evolution rate was correlated with corrosion rates determined by the weight loss. They found that the average rate of hydrogen evolution at temperatures below 100 °C in distilled water was about 0.16 mol/m<sup>2</sup>/yr. The value of 0.29 mol/m<sup>2</sup>/yr at 100 °C given in the Table 1 comes from an older paper of Gould and Evans (1947). A much lower corrosion rates were predicted using hydrogen evolution (0.8 µm/yr – 0.15 molm<sup>-2</sup>yr<sup>-1</sup>) than through weight loss measurements (1.3 µm/yr - molm<sup>-2</sup>yr<sup>-1</sup>). Jelinek and Neufeld (1982) did not find any temperature dependence in the range 60 to 316 °C under the measurement conditions and no catalytic effect of copper.

Simpson and Schenk (Schenk, 1988, Simpson, 1984, Simpson et al., 1985) measured hydrogen evolution in real granitic waters from sites Säckingen and Böttstein and in sodium chloride solutions at temperatures 25, 50 and 80°C and various pH. They used similar chromatographic method of hydrogen quantification as Jelinek and Neufeld (1982). The initial values for hydrogen evolution from real granitic waters achieved very high values about 27.36 mol/m<sup>2</sup>/yr, but after a short time these high values decreased to values given in the Table 2.

**Table 2: Hydrogen evolution from corrosion of iron in real granitic water (Simpson et al., 1985)**

Type of granitic water	25 °C (mol/m <sup>2</sup> /yr)	50 °C (mol/m <sup>2</sup> /yr)	80 °C (mol/m <sup>2</sup> /yr)
Böttstein	0.18	0.98	0.37
Säckingen	0.25	0.51	0.23

The results of hydrogen evolution rate measured by Simpson in dependence of concentration of Cl<sup>-</sup> and two temperatures 80 and 50°C are plotted in the following Fig. 2

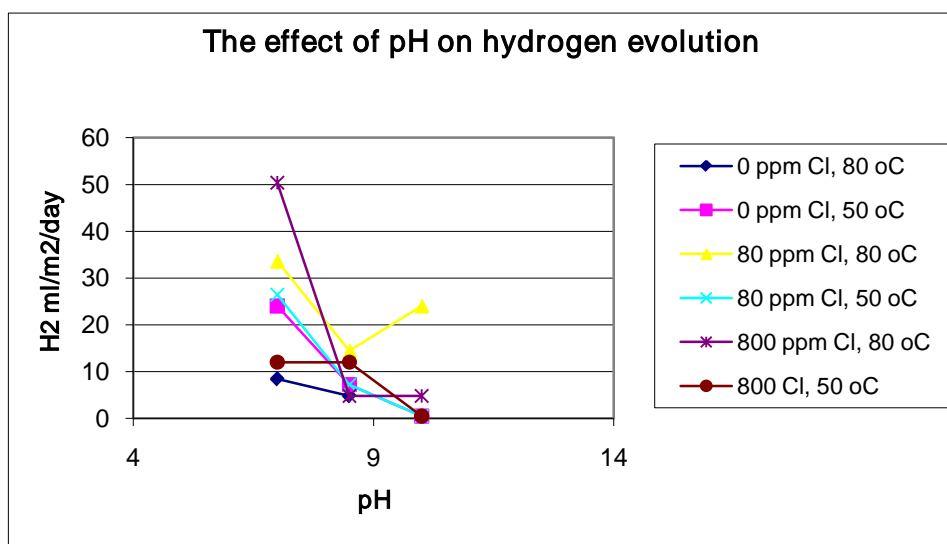


**Figure 2: The effect of pH on hydrogen evolution**

It follows from this figure that hydrogen evolution depends significantly on pH. The effect of temperature does not seem to be significant. The data suggest that there could be some temperature (about 50 °C) at which the hydrogen evolution is maximal. The effect of chloride ions concentration is negligible within the range studied. From a comparison of the data in the table 1 and 2 can be derived that the hydrogen evolution rate of carbon steels in the granitic water could achieve more than five times larger values than in distilled water.



In the same water as Simpson and Schenk (Schenk, 1988, Simpson, 1984, Simpson et al., 1985) from the Böttstein site, Grauer et al. (1991) measured hydrogen evolution at 25°C using equipment based on the measurements of change of volume. They found contrary to the results of Simpson and Schenk (Schenk, 1988, Simpson, 1984, Simpson et al., 1985) that the initial rate of hydrogen evolution is only  $0.07 \text{ molm}^{-2}\text{yr}^{-1}$  under the same compositions of groundwater. This value further decreased to a steady-state value of about  $0.005 \text{ molm}^{-2}\text{yr}^{-1}$  after more than 8000 hours.

At about pH 10, carbon steels evidently passivate and hydrogen evolution is negligible. The similar results on the passivity of carbon steel at higher pH were observed also in the papers of Matsuda et al. (1995) or Fujiwara et al. (2001).

Marsh and Taylor (1988) performed laboratory tests of carbon steel corrosion covered with either crushed granite or bentonite paste to depths of 5, 7.5 or 10 cm in synthetic granitic water. Three types of steel were included in the programme: a forged steel, a cast steel and a low carbon forged steel. Average corrosion rates from experiments, which lasted more than 3 years, were in the range 1.7 to 7.7  $\mu\text{m}/\text{yr}$  in bentonite and 19.2 to 26  $\mu\text{m}/\text{yr}$  in granite. The corrosion rate was determined from weight loss measurements. The corrosion rate of the cast steel was 3-4 times less than the forged steel in bentonite, although there was little to distinguish their behaviour in granite. Only general attack occurred in bentonite. Bentonite specimens were covered by an adherent  $\sim 0.1 \text{ mm}$  layer of bentonite + corrosion product which spalled when it dried out. Visually there was a definite colour change in the bentonite approximately 4.5 cm inward, suggesting this marked region became contaminated with corrosion products. Without the presence of oxygen Marsh and Taylor (1988) strongly suggest that the corrosion rate of carbon steels will be well below  $1 \mu\text{m}/\text{yr}$  ( $0.2 \text{ molm}^{-2}\text{yr}^{-1}$ ) at temperatures below about 50 °C.

Hara et al. (1992) measured hydrogen evolution from carbon steel under various concentration of oxygen. They found that the volume of hydrogen gas generated tends to increase with increasing dissolved oxygen concentration and this tendency was more noticeable after 30 days immersion of specimens than at 14 days immersion. The average hydrogen evolution was about  $0.54 \text{ molm}^{-2}\text{yr}^{-1}$  at the concentration of oxygen of 0.01 ppm, but was more than  $21.2 \text{ molm}^{-2}\text{yr}^{-1}$  at the concentration of 10 ppm of oxygen. They suppose that this is caused by hydrogen evolution in the pits of localized corrosion that occurs in solution with the higher oxygen concentration.

Fujisawa et al. (1997) measured hydrogen evolution from carbon steel wires in mortar water (pH = 12.6), in aqueous solution saturated with calcium hydroxide (pH = 12.8) and in synthetic groundwater with bentonite powder (pH = 8) at three temperature: 15, 30 and 45 °C. The content of oxygen was below 0.06 mg/l. The hydrogen evolution was high at initial period, but was very low after this period. They found a very distinct effect of temperature on hydrogen evolution. The activation energy of corrosion in alkaline water was about 18 kJ/mol. In alkaline (mortar) water, the corrosion rate decreased with time. In contrast, in synthetic groundwater hydrogen gas was generated at a constant rate. The difference in behaviour was explained by the fact that in synthetic groundwater, below pH 9.5, no passive film is formed.

Fujiwara et al. (2001) also observed that for oxygen concentration 100 ppb the evolution of hydrogen from carbon steels increases with an increase of oxygen concentration. They also suppose as Hara et al. (1992) that this is caused by an increase of the localized corrosion area. But under sufficiently reducing conditions, it has been found that generation of hydrogen tends to increase when the oxygen concentration is lower. It was explained as follows: when a passive film is produced on the surface of carbon steel, the generation of hydrogen extremely decreases to the equivalent corrosion rate of  $0.01 \mu\text{m}/\text{year}$  or less. However, under a very low concentration of oxygen the passive film cannot be reproduced sufficiently and therefore the corrosion rate becomes higher. They suppose that air passive film, formed by  $\text{Fe}_2\text{O}_3$ , changes to  $\text{Fe}_3\text{O}_4$  by the dissolution of  $\text{Fe}_2\text{O}_3$  as a complex ion  $\text{HFeO}_2^-$ , which in turn produces  $\text{Fe}_3\text{O}_4$  by reaction with  $\text{H}^+$ .

Smart et al. (2001) used the similar experimental techniques for measuring of hydrogen evolution in the artificial KBS TR 36 groundwater water at 30 and 50 °C as Grauer et al. (1991). He also observed as Grauer et al. (1991) or Simpson and Schenk (Schenk, 1988, Simpson, 1984, Simpson et al., 1985) very high values about  $3.3 \text{ molm}^{-2}\text{yr}^{-1}$  in the beginning of experiments. To investigate the effect of oxide

formation on metal surfaces, they artificially covered carbon steel wires with magnetite or carbonate layers. They found that both films were able to reduce the initial burst in the hydrogen production rate that was observed on pickled metal surfaces. The thick magnetite film specimens showed very little corrosion during the first 100 hours. At all times the rates of hydrogen evolution were below those measured on unfilmed (i.e. pickled) specimens at comparable times. It was found that a more protective layer is formed by magnetite than by iron carbonate.

The addition of 0.1 M  $\text{FeSO}_4$  in groundwater (Smart et al., 2001) resulted in notably increased long-term hydrogen evolution rates, compared to KBS TR 36 groundwater. This was explained by the fact that non-protective layer of  $\text{FeSO}_4$  might be formed on the surface of the carbon steel wires and prevented adherence of protective magnetite layer or alternatively iron sulphate may have caused iron carbonate to precipitate out of the solution, thus leading to a decrease in the pH and formation of a more aggressive environment. Only slight increase of hydrogen evolution was, however, observed with addition of  $\text{K}_2\text{SO}_4$ . An increase of hydrogen evolution by addition of  $\text{FeSO}_4$  could be also explained by reactions of ferrous ions with water leading to hydrogen evolution. This reaction could also explain a significant decrease of pH observed under an addition of  $\text{FeSO}_4$  to the groundwater. An increased acidity itself can also lead to increasing corrosion rate and hydrogen evolution.

The effect of ionic strength and addition of radiolysis products (9 mM  $\text{NH}_3$  or 3 mM  $\text{HNO}_3$ ) or of bentonite to groundwater was also investigated in the paper of Smart et al. (2001). It was observed that ionic strength caused a decrease in the hydrogen production during the first 500 hours compared to more dilute solutions, but in the long term (> 1000 hours) the corrosion rate was approximately an order of magnitude greater than in dilute groundwater. A number of explanations of this effect were formulated in the publication of Smart et al. (2001):

- Increased competition between the formation of magnetite and other less protective iron salts, such as  $\text{FeCO}_3$  or  $\text{FeSO}_4$ .
- Increased availability of anions to form more soluble corrosion products, for example  $\text{FeCl}_2$  instead of  $\text{Fe(OH)}_2$ , and hence reduced ability to form a protective magnetite film
- Incorporation of ions in the magnetite film increasing its conductivity
- Local buffering of pH
- Decrease in the thickness of the protective hard inner magnetite layer due to local buffering of the pH.
- Increased conductivity may enable more efficient electron transfer to occur between the carbon steel and the water.

The effect of an addition of 9 mM  $\text{NH}_3$  or 3 mM  $\text{HNO}_3$  was not significant. They also found that the corrosion rate of cast iron compared to carbon steel is lower. The gas generation rate did not increase significantly after removal of the non-adherent corrosion product, suggesting that hard not-removable inner layer provides the majority of the protection.

Honda et al. (1991) measured the corrosion rate of carbon steel in contact with compacted bentonite. Three specimens with compacted bentonite were placed in a teflon container and filled with water. The bentonite swelled and filled the container. An average corrosion rate was evaluated from the weight loss of specimens. The averaged corrosion rate decreased gradually with increasing test time and was estimated to be in the range 1 to 10  $\mu\text{m}/\text{year}$  ( $0.2 - 2 \text{ molm}^{-2}\text{yr}^{-1}$ ) after period 180 days. Corrosion rates in compacted bentonite were approximately one order of magnitude lower than that in bentonite slurry. Corrosion rates in compacted bentonite mixed with synthetic sea-water were about 2 to 4 times higher than that in compacted bentonite mixed with distilled water. Corrosion rates in compacted bentonite mixed with distilled water were independent of the bentonite bulk density. On the other hand, corrosion rate in the compacted bentonite mixed with synthetic sea-water decreased with an increase in bulk density of the bentonite. Authors suppose that corrosion rates of carbon steel in compacted bentonite were controlled by the diffusion of dissolved oxygen in the compacted bentonite. Only magnetite was found in the case of tests with distilled water and siderite was identified on most of the specimens immersed in the compacted bentonite mixed with synthetic sea-water.

Kozaki et al. (1994) performed corrosion experiments of an iron foil activated by neutrons. The iron foil was placed between two water saturated bentonite specimens and allowed to corrode at 30 °C for periods 16 to 63 days. The corrosion rate was determined from measuring of total activity of  $^{59}\text{Fe}$  released from the foil. No localized corrosion was observed on the surface of the foil. In all the experiments, the values of the corrosion rates in compacted bentonite were on the order of  $1\text{ }\mu\text{m year}^{-1}$ , and no tendency to decrease in the corrosion rates was observed during the period of 60 days.

Anantamula et al. (1987) measured corrosion rate of carbon steel in the packing mixture of 75 wt% of basalt + 25 wt% of bentonite in water containing only 0.1 mg/l of oxygen at 150 °C. The corrosion rates achieved were in the range 23 – 28  $\mu\text{m/year}$  for 1 week experiments and 11 – 14  $\mu\text{m/year}$  for 2 week experiments. These values were at least 7 times lower than corrosion rates of the same types of steel in oxic conditions (95-230  $\mu\text{m/year}$ ).

Xia et al, 2005 performed anaerobic corrosion experiments on carbon steel in contact with compacted bentonite Kunigel V1 of different densities with samples pre-corroded under aerobic conditions. The corrosion rate observed was about 0.1  $\mu\text{m/year}$ .

de Combarieu et al., 2007 has been performed recently corrosion experiments with iron powder. They found that the corrosion rate of iron powder under anaerobic condition in the presence of bentonite in solution was about 1.4  $\mu\text{m/year}$  contrary to 0.66  $\mu\text{m/year}$  without bentonite.

### 1.1.3 Conclusions

It follows from this literature review that hydrogen evolution from anaerobic corrosion of iron metals is not a constant value. A very high value about  $20\text{ molm}^{-2}\text{yr}^{-1}$  can be achieved at the beginning of corrosion until a corrosion layer is formed on the surface of metal. This depends strongly on the conditions of experiments such as: temperature, ionic strength, pH of water, or concentration of oxygen in groundwater. It follows from the results that after some time corrosion rate will decrease to much lower values, certainly below 5  $\mu\text{m/yr}$  corresponding to hydrogen evolution rate lower than  $1\text{ molm}^{-2}\text{yr}^{-1}$ . Most of the experimental results, even suggest that corrosion rate in steady state in anaerobic conditions could be well below 1 or even 0.1  $\mu\text{m/yr}$  ( $0.02 - 0.2\text{ molm}^{-2}\text{yr}^{-1}$ ). The experiments reviewed however, have not been carried out in strictly defined conditions concerning the content of oxygen in water. The results can be doubted therefore from the point that corrosion layers formed on the surface of metal could be more protective than the corrosion layers formed in a repository conditions due to higher content of oxygen in groundwater.

Currently in NRI experiments of carbon steel under in anaerobic box with content of oxygen well below 0.1 ppm at various temperatures are under way. Eh, pH and hydrogen evolution is measured. Other experiments are focused on corrosion of iron powder in contact with compacted, saturated bentonite and also on migration of hydrogen through bentonite. We hope that the results can contribute to explaining some discrepancies observed in literature and provide more reliable data for performance assessments.

### 1.1.4 Literature

Anantamula R.P., Delegard C.H., Fish R.L., (1984), Corrosion behaviour of low-carbon steels in Grande Ronde Basalt groundwater in the presence of basalt-bentonite packing, n Sci Basis for Nuclear Waste Management VII, Mat. Res. Soc. Sym Proc. Vol. 26, p.113

de Combarieu G., Barboux P., Minet Y., Iron corrosion in Callovo-Oxfordian argillite: Form experiments to thermodynamic/kinetic modelling, Physics and Chemistry of the Earth 32, 2007, 346-358

Dunn D.S., Cragnolino G.A., Sridhar N., (2000), An Electrochemical Approach to Predicting Long-Term Localized Corrosion of Corrosion-Resistant High-Level Waste Container Materials, Corrosion-January, Vol. 56, No.1, 90-104

Druyts F., Kursten B., Van Iseghem P., (2001), Corrosion Evaluation of Metallic Materials for Long-Lived HLW/Spent Fuel Disposal Containers, Final report to EDF for the period 1996-1998, SCK.CEN, R-3533, May

Fujisawa R., Cho T., Sugahara K., Takizawa Y., Horikawaa Y., Shiomi T., Hironaga M., The corrosion behaviour of iron and aluminium under waste disposal conditions, Scientific Basis for Nuclear Waste Management XX, MRS Symp. Proc. vol. 465, 1997, p. 675

Fujiwara A., Yasutomi I., Fukudome K., Tateishi T., Fujiwara K., (2000), Influence of Oxygen Concentration and Alkalinity on the Hydrogen Gas Generation by Corrosion of Carbon Steel, Mat. Res. Soc. Symp. Vol. 663, MRS 2001, p. 497, Sci Basis XXIV, Sydney

Grauer R., Knecht B., Kreis P., Simpson J.P., Hydrogen evolution from corrosion of iron and steel in intermediate level waste repositories, Mat. Res. Soc. Symp. Proc. Vol.212, MRS, 1991, Sci. Basis XIV, Boston, str.295

Hara K., Ishikawa H., Honda A., Sasaki N., Influence of Dissolved Oxygen on the Generation Rate of Hydrogen Gas with Corrosion of Carbon Steel, Proceeding of Workshop Gas Generation and Release, OECD Paris 1992, p. 120

Honda A., Teshima T., Tsurudome K., Ishikawa H., Yusa Y., Sasaki N., Effect of compacted bentonite on the corrosion behaviour of carbon steel as geological isolation overpack, Mat. Res. Soc. Symp. Proc. Vol.212, MRS, 1991, Sci. Basis XIV, Boston, str. 287

Jelinek J., Neufeld P., Kinetics of Hydrogen Formation from Mild Steel in Water under Anaerobic Conditions, Corrosion, Vol. 38, No.2, February, 1982

Manaka, Mitsuo Kawasaki, Manabu Honda, Akira, Measurements of the effective diffusion coefficient of dissolved oxygen and oxidation rate of pyrite by dissolved oxygen in compacted sodium bentonite, Nuclear Technology, May 2000, v. 130(2), p. 206-217

Marsh G.P., Taylor K.J., Sharland S.M., Tasker P.W., An approach for evaluation the general and localised corrosion of carbon-steel containers for nuclear waste disposal, in Sci Basis for Nuclear Waste Management X, Mat. Res. Soc. Sym Proc. Vol. 84(1987), str. 227

Matsuda F., Wada R., Fujiwara K., Fujiwara A., An evaluation of hydrogen evolution from corrosion of carbon steel in low/intermediate level waste repositories, MRS, Symp-Proc. Vol. 353, Eds. Murakami T, Ewing R.C. Scientific Basis for Nuclear Waste Management XVIII, 1995, Kyoto, str.719

Platts N., Blackwood D.J., Naish C.C., Anaerobic oxidation of carbon steel in granitic groundwaters: A review of the relevant literature, SKB Technical Report 94-01, February 1994

Puigdomenech I., Ambrosi J-P., Eisenlohr L., Lartigue J-E., Banwart S.A., Bateman K., Milodowski A.E., West J.M., Griffault L., Gustafsson E., Hama K., Yoshida H., Kotelnikova S., Pedersen K., Michaud, Trotignon L., Rivas Perez J., Tullborg E-L., O<sub>2</sub> depletion in granitic media The Rex project, Technical Report SKB TR-01-05, February 2001

Puigdomenech I., Taxen C., Thermodynamic data for copper: Implications for the corrosion of copper under repository conditions, Technical Report SKB TR-00-13, 2000

Puigdomenech I., Trotignon L., Kotelnikova S., Pedersen K., Griffault L., Michaud V., Lartigue J-E., Hama K., Yoshida H., West J.M., Bateman K., Milodowski A.E., Banwari S.A., Rivas Perez J., Tullborg E-L., O<sub>2</sub> consumption in a granitic environment, Mat. Res. Symp. Proc. Vol. 608, MRS, Sci Basis XXIII, Boston, p. 179, 2000

Schenk R., Untersuchungen über die wasserstoffbildung durch eisenkorrosion unter endlagerbedingungen, NAGRA Technischer bericht 86-24, 1988

Simpson J.P., Experiments on Container Materials for Swiss High-Level Waste Disposal Projects Part II, NAGRA Technical report 84-01

Simpson J.P., Schenk R., Hydrogen evolution from corrosion of pure copper, Corrosion Science, Vol. 27, pp. 1365-1370, 1987

Simpson J.P., Schenk R., Knecht B., Corrosion rate of unalloyed steels and cast irons in reducing granitic groundwaters and chloride solutions, Sci Basis for Nuclear Waste Management X, Mat. Res. Soc. Sym Proc. Vol. 50, 1985, Ed- L.O.Werme, p. 429

Smart N.R., Blackwood D.J., Werme L., The anaerobic corrosion of carbon steel and cast iron in artificial groundwaters, SKB Technical Report TR 01-22, July 2001

Smart N.R., Bond A.E., Crossley J.A.A., Lovegrove P.C., Werme L., Mechanical properties of Oxides Formed by Anaerobic Corrosion of Steel, Mat. Res. Soc. Symp. Vol. 663, MRS 2001, p. 477, Sci Basis XXIV, Sydney 2000

Smart N.R., Rance A.P., Fennell P., Werme L., Expansion due to anaerobic corrosion of steel and cast iron: experimental and natural analogue studies, In: Prediction of long term corrosion behaviour in nuclear waste systems. Proceedings of an int. Workshop, Cadarache, France 2002, pp. 280-294

Xia X., Idemitsu K., Arima T., Inagaki Y., Ishidera T., Kurosawa S., Iijima K., Sato H., Corrosion of carbon steel in compacted bentonite and its effect on neptunium diffusion under reducing condition, Applied Clay Science 28, 2005, 89-100

Wiborgh M., Hoglund L.O., Pers K., Gas formation in a L/ILW Repository and gas transport in the host rock, NAGRA Tech. Report 85-17, December 1986

## 1.2 CORROSION UNDER IRRADIATION

In geological repository, containers will be exposed simultaneously to water and radiation. Like corrosion processes, water decomposition under radiation will generate gases like hydrogen, oxygen and hydrogen peroxide. The aim of the study of this second part is to evaluate the impact of radiations on the corrosion processes of carbon steel.

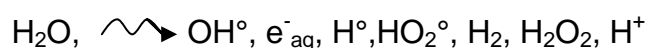
The second part of the progress report is devoted to the state of the art of radiolysis of solutions and of corrosion under radiation.

### 1.2.1 Radiolysis of solutions

Because of radioactive environment, radiolysis of water will occur and produces both radicals and molecular products which could accelerate the corrosion process.

#### 1.2.1.1 PURE WATER RADIOLYSIS

When exposed to radiation ( $\alpha$ ,  $\beta$ ,  $\gamma$ , recoil nuclei), water molecules are excited and ionized, and pure water can degrade as follows:



Where species noted  $^\bullet$  are radicals and  $\text{e}^-_{\text{aq}}$  corresponds to a solvated electron.

The Linear Energy Transfer (LET), corresponding to the loss of energy by unit length in the medium, depends on the type and energy of the ionizing particles. The LET of high energy photons (such as gamma rays) is 0.2 keV per micrometer, while for alpha particle the LET can reach 200 keV/ $\mu\text{m}$  (Pastina, 1999).

The yield of production for each of these species (primary products of radiolysis) depends on nature and intensity of the radiation (Pastina, 1999; Wasselin-Trupin, 2000) (Table 3).

Radiation	G(-H <sub>2</sub> O)	G(e <sup>-</sup> )	G(OH <sup>°</sup> )	G(H <sup>°</sup> )	G(H <sub>2</sub> )	G(H <sub>2</sub> O <sub>2</sub> )	G(H <sub>2</sub> O)
Gamma rays	1.08	2.63	2.72	0.55	0.45	0.68	0.008
Alpha rays	3.9	0.33	0.3	0.1	1.8	1.67	0.13

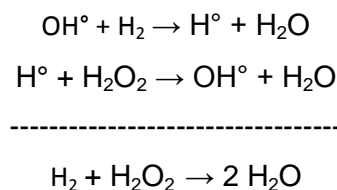
Table 3: Yields of primary species (Pastina, 1997)

Under continuous radiation conditions, the concentrations of radiolysis products depend on LET values. For high LET values, radicals yields are low and molecular species yields are high (Allen, 1961), while for low LET, radicals are preferentially formed.

The primary products undergo reactions (Ershov, 2008) with each other resulting in steady-state concentrations of both radicals and molecular species depending on dose rate, temperature and solution composition.

When irradiated with low LET, such as X-rays or gamma rays, pure degassed water gives almost no products (because of radical recombinations, water is formed), the amount of which of them remains at a very low steady state concentration. For high LET such as alpha rays, pure water decomposition occurs with the formation of hydrogen, hydrogen peroxide and molecular hydrogen. When water contains

oxygen, decomposition occurs whatever the LET value. If hydrogen is present in pure water, the water decomposition is suppressed. This behaviour is linked to the series of reactions involved in the chain reaction proposed by Allen (Allen, 1961) which can be summarized as:



#### 1.2.1.2 RADIOLYSIS PRODUCTS PROPERTIES

Some radiolysis products have acido-basic properties ( $\text{H}^\bullet$ ,  $\text{OH}^\bullet$ ,  $\text{H}_2\text{O}_2$ ,  $\text{HO}_2^\bullet$ ). Their acidity constants have been determined and gathered in Table 4.

equilibrium	pKa – 30°C
$\text{H}_2\text{O} = \text{H}^+ + \text{OH}^-$	13.85
$\text{HO}_2^\bullet = \text{O}_2^- + \text{H}^+$	4.8
$\text{H}_2\text{O}_2 = \text{HO}_2^- + \text{H}^+$	11.62
$\text{OH}^\bullet = \text{O}^- + \text{H}^+$	11.62
$\text{H}^\bullet = \text{e}_{\text{aq}}^- + \text{H}^+$	9.6

Table 4: Acido-basic equilibria (Elliot, 1994)

The radiolysis products range from oxidizing ( $\text{OH}^\bullet$ ,  $\text{H}_2\text{O}_2$ ,  $\text{O}_2^-$ ,  $\text{HO}_2^\bullet$  and  $\text{O}_2$ ) to reducing ( $\text{e}_{\text{aq}}^-$ ,  $\text{H}^\bullet$  and  $\text{H}_2$ ) (Nielsen and Jonsson, 2008). These species, even at low concentrations, may determine the aqueous redox conditions strongly influencing corrosion kinetics (Pastina, 1999).

Redox reactions	Potential /ENH	Medium	References
$\text{OH}^\bullet + \text{e}_{\text{aq}}^- + \text{H}^+ = \text{H}_2\text{O}$	2.72 V	In acidic conditions	(Spotheim-Maurizot et al., 2008)
$\text{OH}^\bullet + \text{e}_{\text{aq}}^- = \text{OH}^-$	1.9 V	In neutral conditions	(Spotheim-Maurizot et al., 2008)
$\text{e}_{\text{aq}}^- + \text{H}^+ = \text{H}^\bullet$	- 2.31 V	In acidic conditions	(Pastina, 1997)

Table 5: Redox properties of some radiolysis products

#### 1.2.1.3 INFLUENCE OF EXPERIMENTAL CONDITIONS

The steady state concentration of a radiolysis product will depend on its radiolysis production rate (constant at a constant dose rate) and on chemical decomposition rates which are very sensitive to aqueous environments such as pH, temperature and chemical additives (Buxton, 1988). Once generated, the primary products undergo further chemical reactions with each other and also with water molecules

and other chemical species present in solution (such as pH- or redox-controlling agents). Therefore, the solution chemistry would change with time (Lapuerta, 2007). The presence of dissolved species or a change in chemical environment affects the concentration of  $\text{H}_2\text{O}_2$  and  $\text{H}_2$  mainly through interactions with radicals  $e_{\text{aq}}^-$  and  $\text{OH}^\bullet$  (Ross, 1979).

#### a Dose rate

In the beginning of the exposure, the amount of radicals increases with radiation dose rate. But, because of the differences in kinetics of recombination reactions (Ross, 1994), a high dose rate induces an increase of molecular products, a decrease of radicals amounts and finally should conduct to water decomposition. Joseph et al. (Joseph, 2008) have shown that for a given pH the steady-state concentrations have a square root dependence on dose rate.

#### b Temperature

The diffusion in solution of primary radiolysis product is enhanced by temperature. Therefore, for high temperature the amount of radicals is high because of limited recombination reactions.

#### c Solution composition

If the water contains a few ppm of dissolved oxygen, the reducing species  $e_{\text{aq}}^-$ ,  $\text{H}^\bullet$ , are rapidly converted to  $\text{HO}_2^\bullet$  and  $\text{O}_2^-$  respectively. In the case of oxygenated water, the concentrations of  $\text{H}_2$  and  $\text{H}^\bullet$  decreased and the most abundant species are  $\text{O}_2$  and  $\text{H}_2\text{O}_2$ . The presence of dissolved  $\text{O}_2$  while radiation fields endures, will lead to a significant increase in the production of radiolytic oxidant. At pH 6, and a dose rate of 25Gy/s (gamma rays), the steady-state concentration of  $\text{H}_2$  and  $\text{H}_2\text{O}_2$  in aerated solutions reached  $2.6 \cdot 10^{-5} \text{ mol/l}$  while it remains below the detection limit level in deaerated solutions. The concentration of  $\text{H}_2\text{O}_2$  was also below the detection limit in deaerated solutions whereas, in aerated solutions, this concentration quickly reached a steady-state concentration of  $0.9 \cdot 10^{-4} \text{ mol/l}$  (Joseph, 2008).

The steady-state concentrations of water decomposition products are nearly independent of pH in the range 5-8. However raising pH above 10 significantly increases  $[\text{H}_2\text{O}]$  and  $[\text{H}_2]$  at the expenses of  $[\text{OH}^\bullet]$  and  $[e_{\text{aq}}^-]$ . The concentration of hydrogen peroxide after 5h irradiation (2.5Gy/s) was closed to  $3 \cdot 10^{-5} \text{ mol/l}$  and those of hydrogen was  $2 \cdot 10^{-4} \text{ mol/l}$  (Joseph, 2008; Yakabuskie, 2010). At  $\text{pH} > 10$ , the production of oxygen becomes significant but at a finite rate.

When carbonate is present, as in bentonite porewater (Table 1),  $\text{OH}^\bullet$  will be quantitatively converted into  $\text{CO}_3^{\bullet-}$ , this being also a strong oxidant ( $E_0$  (NHE) = 1.9V and 1.59V respectively) (Nielsen, 2008). Fattahi et al (Fattahi et al., 1992) have reported an increase (factor 2) of hydrogen peroxide production for clay solution compared to pure water.

## 1.2.2 Radiolysis modelling

Modelling of radiolysis processes can be obtained with different codes. CHEMSIMUL is a computer program system for simulation of chemical kinetics (Rasmussen, 1984) is useful for the simulation of radiolysis processes.

Kinetics constant rates laws are obtained in RATES data base (Ross, 1994) and completed by literature review (Buxton, 1988; Ershov, 2008). An example of input data is given in annex 2.

An illustration of the capabilities of this code is given on figures 3 and 4. In pure deaerated water, the production of hydrogen increases with the dose rate and the duration of radiation (total dose). Fig. 4 shows the differences of hydrogen production under radiation for two solutions: pure water and solution containing carbonate.



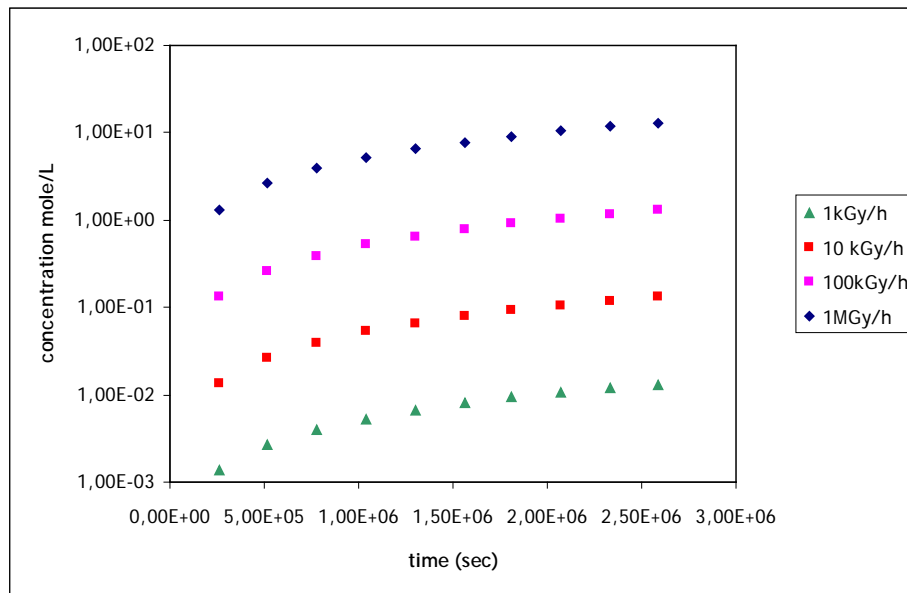


Figure 3: Hydrogen production by irradiated water as a function of dose rate

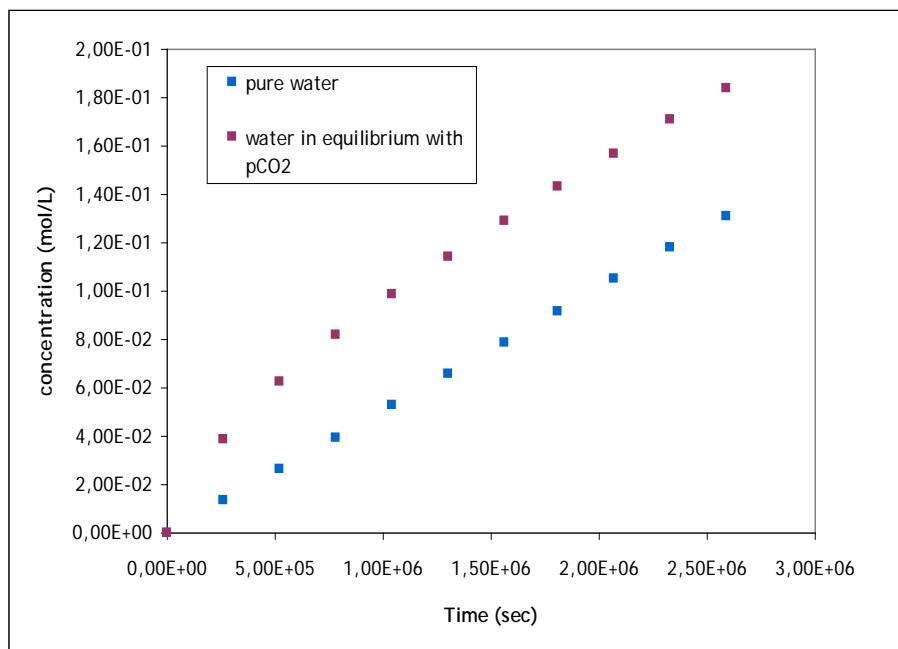


Figure 4: Influence of carbonate on hydrogen production – dose rate = 10kGy/h

### 1.2.3 Influence of radiation on corrosion

The overall redox conditions are established by interactions between reactive radiolysis products, the steel surface and corrosion products produced by these reactions (Joseph, 2008).

Numerous oxidizing and reducing products are produced, all of which can affect the oxidation potential and carbon steel corrosion (Fig. 5).

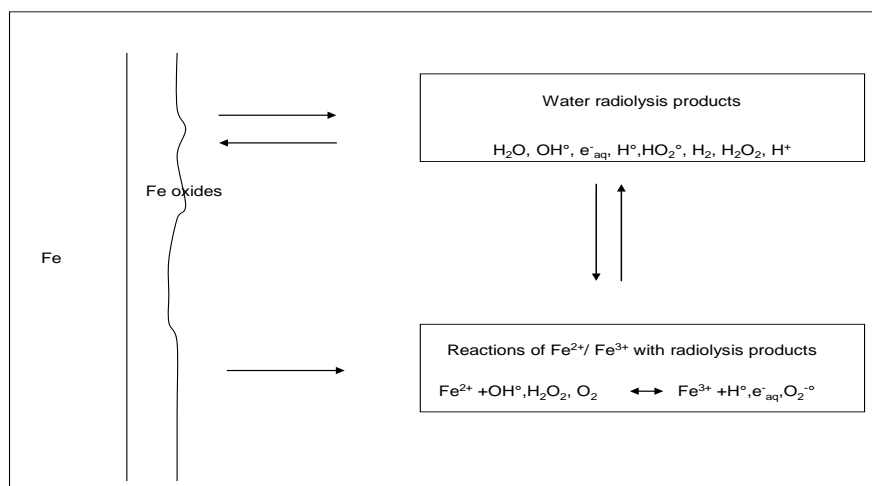


Figure 5: An example of reactions occurring at the interface of carbon steel solution under irradiation (from(Zhang et al., 2007)).

Several papers have put in evidence enhanced corrosion of different materials under charged particle radiations; ceramics, zircaloy and other metals (Burns, 1983; Ishigure, 1980; Lapuerta et al., 2005; Lillard, 2000).

The influence of ionizing radiation on corrosion of metals has been studied only to a limited extent, and the mechanism by which the radiation affects corrosion kinetics has not been established (Daub 2009). The observed effects of ionizing radiation on the corrosion of metals are conflicting and many key questions remain unanswered.

Literature reports some studies on the corrosion processes in primary coolant water of nuclear power plants (Daub, 2008; Pastina, 1999). To limit the corrosion processes in primary coolant water in nuclear reactors, an excess of molecular hydrogen is dissolved in this water. Molecular hydrogen will prevent the accumulation of oxidants products such as oxygen and hydrogen peroxide, which are responsible for the corrosion of the primary system (Pastina, 1999). The molecular hydrogen participates to a chain reaction which recombines H, OH and H<sub>2</sub>O<sub>2</sub> back to water (Allen chain).

An experimental study (Marsh et al. 1988) on the corrosion of carbon steel in presence and absence of radiation (dose rate up to 10<sup>2</sup> rad/h) has been conducted in synthetic granitic waters (pH = 9.4). Without irradiation, the rate of general corrosion was less than 0.1 µm/y. In the same environment, with a maximum gamma dose rate of 10<sup>5</sup>rad/h, the general corrosion rate was fairly constant at 3 µm/y at least up to 5236 h (duration of the experiment). As on unirradiated samples, no localized corrosion was observed.

More recently, Daub (Daub, 2009) have shown that the corrosion behaviour for a pH of 10.6 under gamma-irradiation at room temperature could be simulated well by exposing the steel to solutions containing an equivalent concentration of hydrogen peroxide. More, these authors observed that the addition of H<sub>2</sub>O<sub>2</sub> in multiple steps matches the change in corrosion potential under irradiation. In the conditions of the experiment, Daub (2009) concludes that H<sub>2</sub>O<sub>2</sub> is the key radiolysis product.

Lapuerta et al. (Lapuerta et al., 2005; Lapuerta, 2007; Lapuerta, 2006) have studied corrosion of iron under proton radiation in atmospheric conditions and in aqueous medium.

In atmosphere, without radiation, the corrosion kinetics is maximum for a relative humidity of 80-90%. Under radiation, the maximum of corrosion is observed for a humidity of 45%. For higher humidity content, the corrosion rate decreases. The results show that radiation influences corrosion only when water (vapour) and oxygen are simultaneously present.

As in atmospheric conditions, under radiation, iron corrosion in solution is enhanced when oxygen is present (corrosion is twice more significant in aerated medium than in deaerated one). Moreover, Lapuerta et al. (Lapuerta, 2007) has shown that the radicals produced by water radiolysis participate to the corrosion processes (together with hydrogen peroxide).

Smart et al. (Smart, 2008) have conducted experiments designed to investigate the effect of gamma radiation on the corrosion of steel in repository environments.

Tests were carried out, in anaerobic environments, on carbon steel wires for 2 temperatures (30°C and 50°C), 2 dose rates (11Gy/h, 300 Gy/h) in 2 different artificial groundwaters (Modified Allard GW, bentonite equilibrated GW).

Radiation was found to enhance the corrosion rates at both dose rates but the greatest enhancement occurred at the higher dose rate. The presence of gamma radiation increases the anaerobic corrosion of carbon steel in artificial groundwaters. At 11Gy/h, the increase only lasts for 7 000 hours, but at 300Gy/h, the enhancement is longer lasting. The enhancement of the corrosion rate is higher in “Allard water” where a 30 fold increase was observed than in “bentonite water” which has a higher ionic strength and a higher initial pH, where the radiation-induced enhancement was 10-20 times. The corrosion rate value estimated on the basis of hydrogen release is closed to values obtained by Marsh and Taylor (3 µm/y compared to less than 0.1µm/year without radiation). No localised attack was observed.

The variation of pH of solutions after irradiation experiments is less than 0.1 (Marsh and Taylor, 1988; Smart, 2008).

Fujita et al. (Fujita et al., 2000; Fujita et al., 2001) have observed a corrosion rate in pure deaerated water under a dose rate of 0.55kGy/h for 300, 600 and 900h six times larger as that under a non-irradiated condition.

The main corrosion product is magnetite,  $\text{Fe}_3\text{O}_4$ , but there was some evidence of higher oxidation state oxy hydroxides ( $\text{Fe}_2\text{O}_3$ ,  $\text{FeOOH}$ ) under high dose rate (Daub, 2009; Xu et al., 2008).

Smart (Smart, 2008) mentioned that the corrosion product formed under high dose rate (300Gy/h) has a different colour to the specimen obtained at 0 and 11Gy/h. Fujita et al. have observed through X-Ray Diffraction analysis a preferential dissolution of a specific (110) plane, which potentially triggers an occurrence of the pitting corrosion and an incipient crack.

#### 1.2.4 Conclusion

Studies devoted to the corrosion of iron under radiation seem indicate that the corrosion of carbon steel is enhanced under irradiation. But uncertainties still remain about the factor of enhancement. Most of these studies are conducted in pure water and the influence of dissolved species on corrosion under species is not currently studied. Generally, authors have observed the formation at the interface steel/solution of magnetite together with oxy-hydroxide. It is necessary to examine the influence of this last oxide on the corrosion rate.

At least, no unanimity was obtained towards the state of the surface of carbon steel corroded under irradiation. Is it a generalized or localized corrosion (cracks)?

The experimental program developed will bring some answer to those questions.

#### 1.2.5 Literature:

Allen, A.O., 1961, The radiation chemistry of water and aqueous solutions, *in* Nostrand, V., ed.: New York.

Burns, W.G.M., W. R.;Walters, W. S., 1983, The  $[\lambda]$  irradiation-enhanced corrosion of stainless and mild steels by water in the presence of air, argon and hydrogen: Radiation Physics and Chemistry (1977), v. 21, p. 259-279.

- Buxton, G.V.G., Clive L.;Helman, W. Phillips;Ross, Alberta B., 1988, Critical Review of rate constants for reactions of hydrated electrons, hydrogen atoms and hydroxyl radicals ( $\cdot\text{OH}/\cdot\text{O}^{\sup -}$ ) in Aqueous Solution: Journal of Physical and Chemical Reference Data, v. 17, p. 513-886.
- Daub, K.Z., X.; Noël, J. J.;Shoesmith D.;Wren, J. C., 2008, Effect of gamma radiation on steel corrosion, *in* Curran Associates, I., ed., 9th Annual Conference of the Canadian Nuclear Society and 32nd CNS/CNA Student Conference: Toronto -Ontario, CANADA.
- Daub, K.Z., X.; Noël, J. J.;Wren, J. C., 2009, Effects of  $[\gamma]$ -radiation versus  $\text{H}_2\text{O}_2$  on carbon steel corrosion: *Electrochimica Acta*, v. In Press, Corrected Proof.
- Elliot, A.J., 1994, rate constants and G-values for the simulation of the radiolysis of light water over the range 0-300°C, *in* 11073, A.-. ed.
- Ershov, B.G.G., A. V., 2008, A model for radiolysis of water and aqueous solutions of  $\text{H}_2$ ,  $\text{H}_2\text{O}_2$  and  $\text{O}_2$ : *Radiation Physics and Chemistry*, v. 77, p. 928-935.
- Fattahi, M., Houée-Levin, C., Ferradini, C., and Jacquier, P., 1992, Hydrogen peroxide formation and decay in  $[\gamma]$ -irradiated clay water: *International Journal of Radiation Applications and Instrumentation. Part C. Radiation Physics and Chemistry*, v. 40, p. 167-173.
- Fujita, N., Matsuura, C., and Saigo, K., 2000, Irradiation-enhanced corrosion of carbon steel in high temperature water -- in view of a cell formation induced by  $[\gamma]$ -rays: *Radiation Physics and Chemistry*, v. 58, p. 139-147.
- , 2001, Radiation-induced preferential dissolution of specific planes of carbon steel in high-temperature water: *Radiation Physics and Chemistry*, v. 60, p. 53-60.
- Ishigure, K.F., N.;Tamura, T.;Oshima, K., 1980, Effect of gamma radiation on the release of corrosion products from carbon steel and stainless steel in high temperature water. [PWR; BWR]: Journal Name: Nucl. Technol.; (United States); Journal Volume: 50:2, p. Medium: X; Size: Pages: 169-177.
- Joseph, J.M.S.C., Byung;Yakabuskie, Pam;Clara Wren, J., 2008, A combined experimental and model analysis on the effect of pH and  $\text{O}_2(\text{aq})$  on  $[\gamma]$ -radiolytically produced  $\text{H}_2$  and  $\text{H}_2\text{O}_2$ : *Radiation Physics and Chemistry*, v. 77, p. 1009-1020.
- Lapuerta, S., Moncoffre, N., Millard-Pinard, N., Mendes, E., Corbel, C., and Crusset, D., 2005, use of ion beam analysis techniques to characterise iron corrosion under water radiolysis *Nuclear Instruments and Methods in Physics Research Section B: Beam Interactions with Materials and Atoms*, v. 240.
- Lapuerta, S.M.-P., N; Moncoffre, N.;Bererd, N.; Jaffrezic, H.; Brunel, G.;Crusset, D.;Mennecart, Th, 2007, Origin of the hydrogen involved in iron corrosion under irradiation: *Surface and Coatings Technology*, v. 201, p. 8197-8201.
- Lapuerta, S.M., N.;Bererd, N.; Jaffrezic, H.;Millard-Pinard, N; Crusset, D., 2006, Ion beam analysis of the effect of  $\text{O}_2$  and  $\text{H}_2\text{O}$  on the oxidation of iron under irradiation: *Nuclear Instruments and Methods in Physics Research Section B: Beam Interactions with Materials and Atoms*, v. 249, p. 470-473.
- Lillard, R.S.P., D. L.;Butt, D. P., 2000, The corrosion of materials in water irradiated by 800 MeV protons: *Journal of nuclear materials*, v. 278, p. 277-289.
- Marsh, G.P., and Taylor, K.J., 1988, An assessment of carbon steel containers for radioactive waste disposal: *Corrosion Science*, v. 28, p. 289-320.

- Nielsen, F.L., Karin;Jonsson, Mats, 2008, Simulations of H<sub>2</sub>O<sub>2</sub> concentration profiles in the water surrounding spent nuclear fuel: *Journal of nuclear materials*, v. 372, p. 32-35.
- Pastina, B., 1997, Etude sur la radiolyse de l'eau en relation avec le circuit primaire de refroidissement des réacteurs nucléaires à eau sous pression: Orsay, Partis XI
- Pastina, B.I., J.; Hickel, B., 1999, The influence of water chemistry on the radiolysis of the primary coolant water in pressurized water reactors: *Journal of nuclear materials*, v. 264, p. 309-318.
- Rasmussen, O.L.B.E., 1984, Chemsimul - a program package for numerical simulation of chemical reaction systems. , *in* Rissô National Laboratory, D., ed., Volume Technical Report Risö-R-395 (ENG)
- Ross, A.B., Mallard W.G., Helman W.P., Buxton G.V., Huie P. E., Neta P., 1994, Solution Kinetics Database - Version 2.0 NIST Gaithersburg USA, *in* NDRL-NIST, ed.
- Ross, A.B., Neta P., 1979, rate constants for reactions of inorganic radicals in aqueous solutions, p. 58p.
- Smart, N.R.R., A. P.;Werme, L. O., 2008, The effect of radiation on the anaerobic corrosion of steel: *Journal of nuclear materials*, v. 379, p. 97-104.
- Spotheim-Maurizot, M., Mostafavi, M., Douki, Y., and Belloni, J., 2008, Radiation Chemistry, l'actualité chimique, EDP Sciences.
- Wasselin-Trupin, V., 2000, Processus primaires en chimie sous rayonnement. Influence du Transfert d'Energie Linéique sur la radiolyse de l'eau. : Orsay, Paris XI.
- Xu, T., Senger, R., and Finsterle, S., 2008, Corrosion-induced gas generation in a nuclear waste repository: Reactive geochemistry and multiphase flow effects: *Applied Geochemistry*, v. 23, p. 3423-3433.
- Yakabuskie, P.A.J., Jiju M.;Clara Wren, J., 2010, The effect of interfacial mass transfer on steady-state water radiolysis: *Radiation Physics and Chemistry*, v. In Press, Accepted Manuscript.
- Zhang, X., Xu, W., Shoesmith, D.W., and Wren, J.C., 2007, Kinetics of H<sub>2</sub>O<sub>2</sub> reaction with oxide films on carbon steel: *Corrosion Science*, v. 49, p. 4553-4567.

## Annexes

Table 1: Composition of clay porewater for 3 different dry densities

Dry density (kg/cm <sup>3</sup> )	1300	1600	1900
Porosity	0.122	0.044	0.019
Log PCO <sub>2</sub>	- 3.42	-3.47	-3.65
Na (M)	0.183	0.207	0.254
K (M)	0.0027	0.0031	0.0037
Mg (M)	0.01	0.012	0.015
Ca (M)	0.0092	0.0098	0.012
Sr (M)	8.1 E-5	8.6 E-5	1.1 E-4
Cl (M)	0.0181	0.0618	0.17
SO <sub>4</sub> (M)	0.102	0.095	0.071
Cinorg (M)	8.9 E-4	8 E-4	5.5 E-4
F (M)	2.2 E-4	2.2 E-4	1.9 E-4
Si (M)	1.8 E-4	1.8 E-4	1.8 E-4

## CHEMSIMUL: .dat

### \$chemical reactions

#### \* équilibres acide base

\*H2O !pke=15.75 !molecule d'eau=55.5  
 RE1:  $\text{H}_2\text{O} + \text{H}_2\text{O} = \text{OH}[-] + \text{H}_3\text{O}[+]$ ; A=2.36e-5  
 RE2:  $\text{OH}[-] + \text{H}_3\text{O}[+] = \text{H}_2\text{O} + \text{H}_2\text{O}$ ; A=1.3e11

...

#### \* reactions with e-aq

RE15:  $\text{E}[-] + \text{E}[-] = \text{H}_2 + \text{OH}[-] + \text{OH}[-]$ ; A=5.5E9  
 RE16:  $\text{E}[-] + \text{H} = \text{H}_2 + \text{OH}[-]$ ; A=2.54E10

..

#### \*reactions with radical H

RE25:  $\text{H} + \text{O}[-] = \text{OH}[-]$ ; A=1E10

...

#### \* reactions with radical OH

RE33:  $\text{OH} + \text{H}_2 = \text{H}_2\text{O} + \text{H}$ ; A=6e7  
 RE34:  $\text{OH} + \text{OH} = \text{H}_2\text{O}_2$ ; A=5.5E9

.....

#### \* reactions with radical HO2

RE40:  $\text{HO}_2 + \text{O}_2[-] = \text{HO}_2[-] + \text{O}_2$ ; A=9.7e7  
 RE41:  $\text{HO}_2 + \text{HO}_2 = \text{H}_2\text{O}_2 + \text{O}_2$ ; A=8.3e5

#### \* reactions with radical O[-]

RE42:  $\text{O}[-] + \text{H}_2 = \text{H} + \text{OH}[-]$ ; A=1.E8

...

#### \* reactions with radical O3[-]

RE50:  $\text{O}_3[-] = \text{O}_2 + \text{O}[-]$ ; A=2.6E3

....

#### \* reactions with carbonates

RE63:  $\text{HCO}_3[-] + \text{OH} = \text{CO}_3[-] + \text{H}_2\text{O}$ ; A=8.5e6

...

#### \* reactions with .... Solution species (sulfate, nitrate..)

### Solution composition

\$concentrations déduites de Jchess eau-oxygene

con(H3O[+])=0  
 con(HCO3[-])=2.2e-6  
 con(H2CO3)=1.0735e-5  
 con(H2O)=55.5e0  
 con(OH[-])=0  
 con(O2)=2.52e-4  
 con(CO3[--])=4.71e-11

### \$integration

eps=1.0e-5  
 \*fststp=5.0e-7  
 \*hmax=5.0e-3  
 tend=1.296e6  
 \*jt=

### \$output control

\*derivative(O2)  
 dig=3  
 mathinfo  
 diffeq  
 linele=80  
 prints=110  
 radprs=110  
 \*prntonly(H2O2,H2)  
 \*save

### \$irradiation

G(H)=0.5  
 G(OH)=1  
 G(H2O2)=1.2  
 G(E[-])=0.74  
 G(H2)=0.88  
 G(H3O[+])=0.74  
 G(HO2)=0.2  
 G(H2O)=-4.54  
 \*nrr  
 RADTIME=1.296e6  
 \*ttrain  
 TOTALDOSE=1.26e6